

No.17

FEBRUARY 1999.

CONTENTS

	pg.
Solutions to the Questions in Issue No.16	369
Regular Cylindrical Bihelix Braids	378

A quarterly publication
for
the braiding artisan

Resale of this publication or copies thereof
is strictly prohibited

Copyright ©1999 by :

{ A.G. Schaake; 21 Sundown Cresc.; Hamilton; New Zealand.
D. Van Tassel; Box 335; Craig, Co 81626-0335; U.S.A.
F.J.M. Masurel; Ganzenzijde 4; 2317XG Leiden; Nederland.

All rights reserved. No part of this publication may be reproduced, stored in a retrieval system, or transmitted, in any form or by any means, electronic, mechanical, photo-copying, recording, or otherwise, without prior written permission.

This publication is available to braiding artisans only.

Copies may be obtained from :

A.G. Schaake,
21 Sundown Cresc.,
Hamilton,
New Zealand.

Solutions to the Questions in Issue No. 16

Question on pp. 351 – 352.

This question is a very important one since after solving the various sub-questions a multitude of questions in fields other than braiding, but *possibly* related, should present themselves. In the near future we shall present one of those questions in what therefore has to be called a “sideline” article which is associated with SE (*spongiform encephalopathy*) to which BSE (*mad cow disease*), CJD (*Creutzfeldt-Jacob disease*), Kuru, FFI (*fatal familial insomnia*) and GSS (*Gerstmann-Sträussler-Scheinker disease*) belong.

The following solutions should be carefully studied and be thoroughly comprehended since they not only clearly demonstrate the fallacious approach to knots and braids by the topological knot theorists (their theory is in relation to knots and braids a mathematical fallacy), but are of fundamental importance to knots and braids.

Although the fundamental properties of twist have been discussed in Issue No. 16 on pg. 352 we like to recall the two fundamental arrangements depicted in Fig. 315.

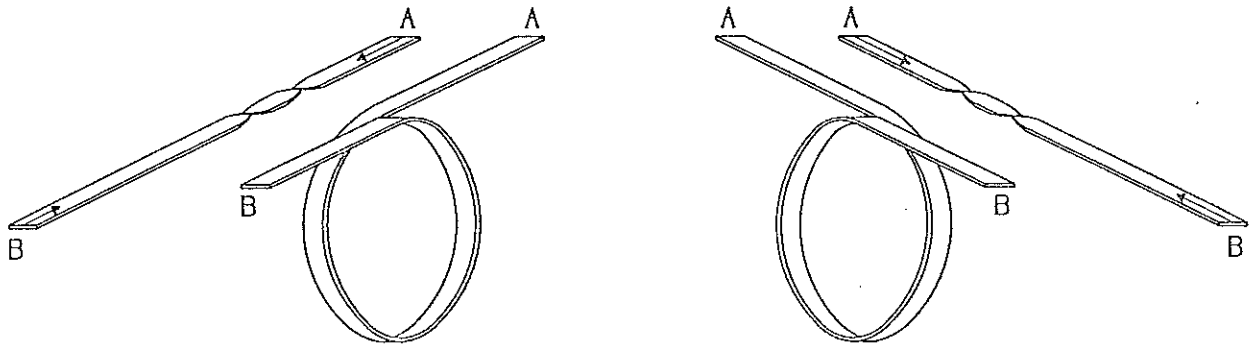


Fig. 315 — Two right helix and two left helix half twists and their equivalent loops.

The left-hand drawing clearly indicates that the loop formed creates two half twists with a **left** helix which cancel the two half twists with the right helix in the string depicted at the extreme left-hand side. Similarly the right-hand drawing indicates that the loop formed creates two half twists with a **right** helix which cancel the two half twists with the left helix in the string depicted at the extreme right-hand side. Consequently if we form in the string depicted at the extreme left a loop by bringing **A** to the **right** of **B** instead of to the left, we finish up with a loop and two additional half twists with a **right** helix, hence a loop and four half twists with a right helix. Similarly, if we form in the string depicted at the extreme right a loop by bringing **A** to the **left** of **B** instead of to the right, we finish up with a loop and two additional half twists with a **left** helix, hence a loop and four half twists with a left helix.

We can now compile the tables on pg. 371. Each table deals with its indicated number of half twists (whether with a left helix or right helix) in a piece of string. The left-hand part of these tables deals with the placing of string “ends” **A** and **B** in their relative positions which immediately decrease the number of half twists with the formation of the first loop, and the right-hand part of these tables deals with the placing of string “ends” **A** and **B** in their relative positions which first create **two additional** half twists with the formation of the first loop. In these tables **M** indicates a Regular Möbius Braid whereas **C** indicates a Regular Cylindrical Braid. The number of loops are the number of parts in the braids concerned. In the first table the **-1 Half Twists** indicates that its

associated helix is of the opposite type to the original half twist in the string. We have an x -parts Regular Knot when with x loops the associated number of half twists is zero, and we have an x -parts Regular Möbius Knot when with x loops the associated number of half twists is x . Let's have a look at an Example in order to clarify this.

Example : A string with 8 half twists.

In the left-hand part of the table for 8 half twists we obtained the useful entry : 4 loops + 0 half twists together with the indication C . Since there are no half twists left we have a 1-string Regular Cylindrical Braid of 4-parts. The number of bights can be made any number which is coprime with 4.

In the right-hand part of this table for 8 half twists we obtained two useful entries: one entry specifying 4 loops + 4 half twists together with the indication M , hence the braid is a 1-string Regular Cylindrical Braid of $p = p_m = 4$ -parts and a half twist in each part. This braid can be transformed (without interfering with the string-ends and the number of loops) into a 1-string Regular Cylindrical Braid of $p = p_m = 4$ -parts which contains a Matthew Walker section with $\frac{p}{2} = \frac{p_m}{2} = \frac{4}{2} = 2$ -bights and a half twist in each of its $p = p_m = 4$ -parts. This braid can be transformed into a 4-parts Regular Möbius Knot by deleting its Matthew Walker section (and at the same time the half twists). The other entry specifies 6 loops + 0 half twists together with the indication C . Since there are no half twists left we have a 1-string Regular Cylindrical Braid of 6-parts. For the number of bights we can take any number which is coprime with 6.

Fig. 316 shows for each of the in the tables indicated Regular Möbius Knots a grid-diagram (with Matthew Walker section containing p_m half twists) for one of the many possible b_m -values to the right of the grid-diagram of its equivalent Regular Cylindrical Braid with one bight and p_m half twists. The upper two rows and the lower two rows of grid-diagrams are associated with a string in which the half twists have a left helix, respectively a right helix. In these diagrams the Matthew Walker sections are bordered by thick lines.

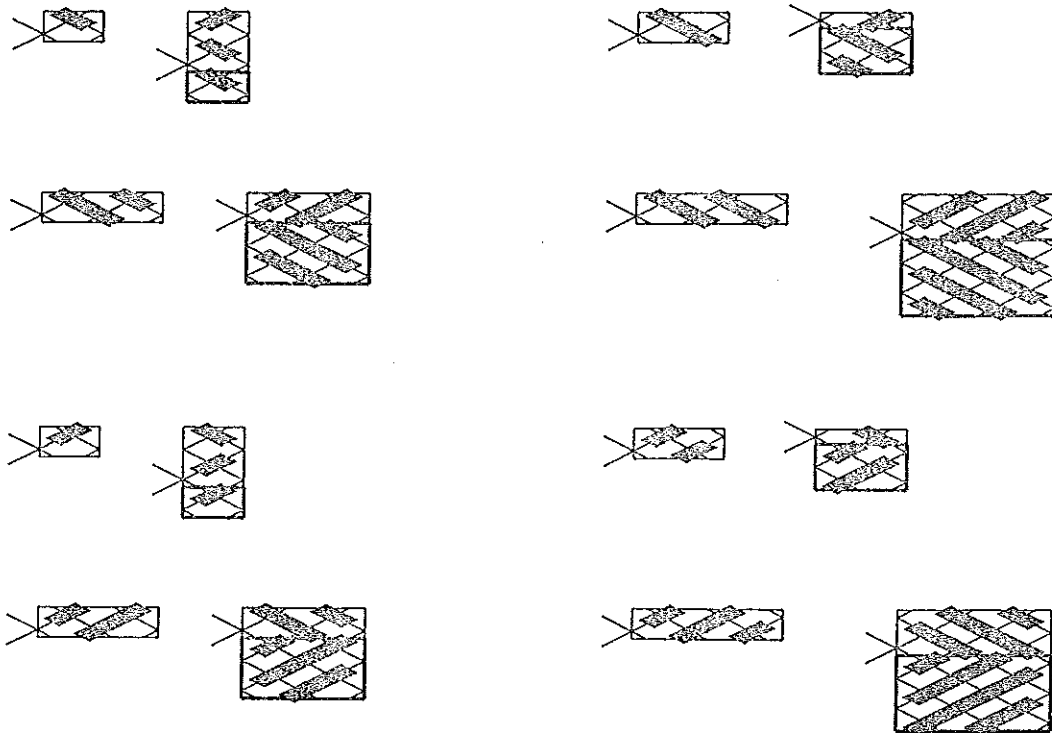


Fig. 316 — Some possible Regular Möbius Knots associated with the table entries.

1 HALF TWIST			
LOOPS + HALF TWISTS		LOOPS + HALF TWISTS	
1	-1 → M	1	3
		2	1

2 HALF TWISTS			
LOOPS + HALF TWISTS		LOOPS + HALF TWISTS	
1	0 → C	1	4
		2	2 → M
		3	0 → C

3 HALF TWISTS			
LOOPS + HALF TWISTS		LOOPS + HALF TWISTS	
1	1 → M	1	5
		2	3
		3	1

4 HALF TWISTS			
LOOPS + HALF TWISTS		LOOPS + HALF TWISTS	
1	2	1	6
2	0 → C	2	4
		3	2
		4	0 → C

5 HALF TWISTS			
LOOPS + HALF TWISTS		LOOPS + HALF TWISTS	
1	3	1	7
2	1	2	5
		3	3 → M
		4	1

6 HALF TWISTS			
LOOPS + HALF TWISTS		LOOPS + HALF TWISTS	
1	4	1	8
2	2 → M	2	6
3	0 → C	3	4
		4	2
		5	0 → C

7 HALF TWISTS			
LOOPS + HALF TWISTS		LOOPS + HALF TWISTS	
1	5	1	9
2	3	2	7
3	1	3	5
		4	3
		5	1

8 HALF TWISTS			
LOOPS + HALF TWISTS		LOOPS + HALF TWISTS	
1	6	1	10
2	4	2	8
3	2	3	6
4	0 → C	4	4 → M
		5	2
		6	0 → C

9 HALF TWISTS			
LOOPS + HALF TWISTS		LOOPS + HALF TWISTS	
1	7	1	11
2	5	2	9
3	3 → M	3	7
4	1	4	5
		5	3
		6	1

10 HALF TWISTS			
LOOPS + HALF TWISTS		LOOPS + HALF TWISTS	
1	8	1	12
2	6	2	10
3	4	3	8
4	2	4	6
5	0 → C	5	4
		6	2
		7	0 → C

11 HALF TWISTS			
LOOPS + HALF TWISTS		LOOPS + HALF TWISTS	
1	9	1	13
2	7	2	11
3	5	3	9
4	3	4	7
5	1	5	5 → M
		6	3
		7	1

12 HALF TWISTS			
LOOPS + HALF TWISTS		LOOPS + HALF TWISTS	
1	10	1	14
2	8	2	12
3	6	3	10
4	4 → M	4	8
5	2	5	6
6	0 → C	6	4
		7	2
		8	0 → C

13 HALF TWISTS			
LOOPS + HALF TWISTS		LOOPS + HALF TWISTS	
1	11	1	15
2	9	2	13
3	7	3	11
4	5	4	9
5	3	5	7
6	1	6	5
		7	3
		8	1

From the tables we see that a string with 1 half twist is a special case and that from a string with $(6n + 1)$ half twists (where n is a positive integer) neither all half twists can be eliminated, nor that the loops can each have a half twist only. The overall results for eliminating (if possible) all half twists in a string may be summarised as follows:

- A string with 1 half twist is a special case and is equivalent to a 1-part Regular Möbius Knot with the opposite helix.
- A string with n half twists (n is a positive integer greater than 1) is equivalent to:
 - (i). An $\frac{n}{2}$ -parts Regular Knot when $\frac{n}{2}$ is a positive integer.
 - (ii). An $\frac{n+4}{2}$ -parts Regular Knot when $\frac{n+4}{2}$ is a positive integer.
 - (iii). An $\frac{n}{3}$ -parts Regular Möbius Knot with the opposite helix when $\frac{n}{3}$ is a positive integer.
 - (iv). An $\frac{n+4}{3}$ -parts Regular Möbius Knot with the opposite helix when $\frac{n+4}{3}$ is a positive integer.

It will be clear that half twists in a piece of string represent dormant braids. It is of special significance that a set number of half twists always represents at least two sets of braids, which for an even number of half twists are genuine Regular Cylindrical Knots, and which for an odd number of half twists, equal to or greater than 5, are prime hybrids between Regular Cylindrical Knots and Regular Möbius Knots (they are Regular Cylindrical Knots with only one half twist in their entire string-run (the Möbius facet)). Depending on the number of half twists there may or may not be one set of prime Regular Möbius Knots. All the knots in a specific set have the same number of parts which is a function of the number of twists, while they may possess various numbers of bights.

We like to stress once again that the relationship between the number of half twists and the knots they represent in dormant form is one of the very fundamental properties of knots. It is really staggering that mathematicians have overlooked and hence ignored this most fundamental property. Although, are it not the obvious and most simple but essential matters of which the academic world is so often totally oblivious? Not for nothing is there the well known saying: "some of the greatest nitwits I have met have been academics".

Question on pg. 364.

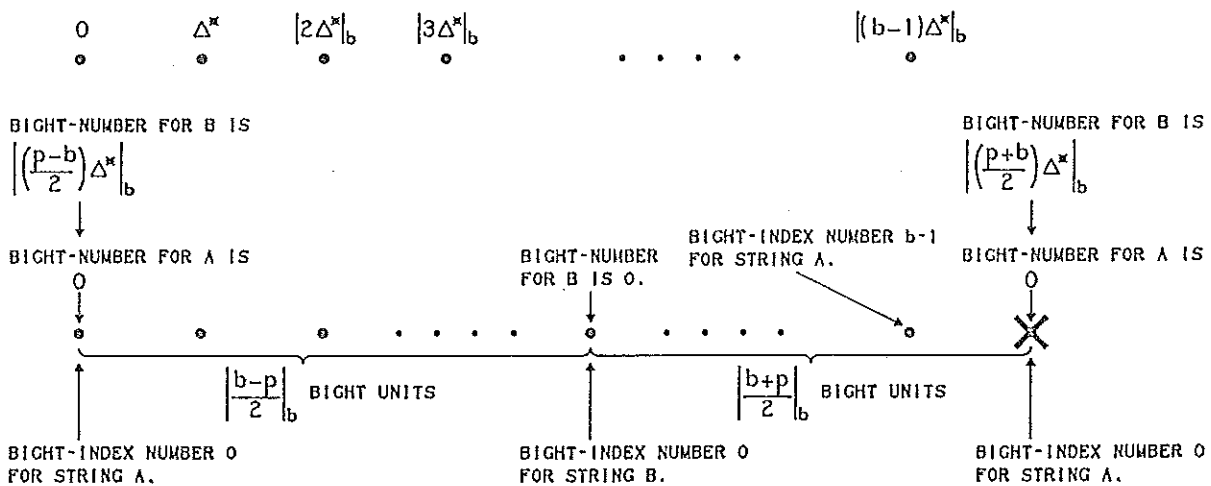


Fig. 317 — The complementary cyclic bight-number schemes for the strings A and B.

Let string-run A be the real string-run and let string-run B be the imaginary string-run. Then the uppermost diagram in Fig. 317 depicts the complementary cyclic bight-number scheme for string A .

The bight-points of string A are also the bight-points of string B , however, the strings A and B start at different bight-points. The bight-point at which the imaginary half-cycle of higher order of string B starts (bight-index number 0 for string B) receives in the complementary cyclic bight-number scheme the bight-number 0. Since $p = p_m$ and $b = b_m$, this bight-point has for string A the bight-index number $\left\lfloor \frac{b-p}{2} \right\rfloor_b$. Hence it lies $\left\lfloor \frac{b-p}{2} \right\rfloor_b$ bight-units to the right of the bight-point at which string A starts, as well as $\left\lfloor \frac{b+p}{2} \right\rfloor_b$ bight-units to the left of this starting point for string A . Let in the complementary cyclic bight-number scheme this starting bight-point of string A have the bight-number x for string B . Then:

$$\begin{aligned}
 2x &= \left\lfloor \left(\frac{p-b}{2} \right) \Delta^* \right\rfloor_b + \left\lfloor \left(\frac{p+b}{2} \right) \Delta^* \right\rfloor_b \\
 &= \frac{1}{2} |(p-b)\Delta^*|_{2b} + \frac{1}{2} |(p+b)\Delta^*|_{2b} \\
 &= \frac{(p-b)\Delta^* + (p+b)\Delta^* + 2sb}{2} \\
 &= \frac{2p\Delta^* + 2sb}{2} \quad \text{where } s = \text{integer.} \\
 x &= \frac{p\Delta^* + sb}{2}. \quad \text{Hence with } \Delta^* = \frac{b \cdot \Delta_{II,1} p - 1}{p}: \\
 x &= \frac{p \cdot \frac{b \cdot \Delta_{II,1} p - 1}{p} + sb}{2} \\
 &= \frac{b \cdot \Delta_{II,1} p - 1 + sb}{2} \\
 &= \frac{b-1}{2}, \quad \text{since } b = \text{odd and } 0 \leq x \leq b-1.
 \end{aligned}$$

Thus we obtain the complementary cyclic bight-number scheme depicted in Fig. 318.

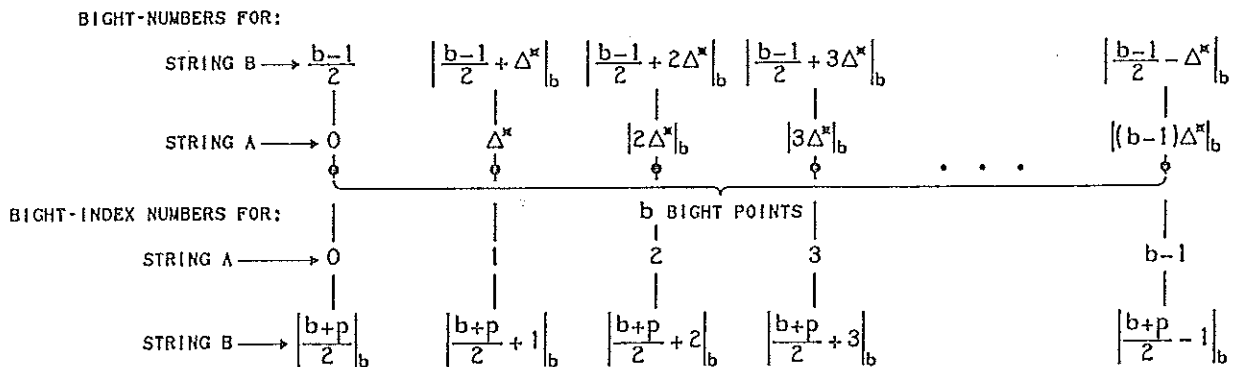


Fig. 318 — The complementary cyclic bight-number scheme for $p = p_m = \text{odd}$ and $b = b_m = \text{odd}$ with $\text{g.c.d.}(p_m, b_m) = 1$.

Let for the imaginary string-run (hence string-run B) $i_y = a^*$ and $i_{p-y} = b^*$ (see Fig. 319). Then:

$$\begin{aligned}
 |i_y + i_{p-y}|_b &= \left| \left| \frac{b-1}{2} + y\Delta^* \right|_b + \left| \frac{b-1}{2} + (p-y)\Delta^* \right|_b \right|_b \\
 &= |b-1 + p\Delta^*|_b \\
 &= |p\Delta^* - 1|_b. \quad \text{Hence with } \Delta^* = \frac{b \cdot \Delta_{II,1} p - 1}{p} :
 \end{aligned}$$

$$\begin{aligned}
 |i_y + i_{p-y}|_b &= \left| b \cdot \Delta_{II,1} p - 1 - 1 \right|_b = |-2|_b \\
 &= b - 2.
 \end{aligned}$$

$i_y + i_{p-y} = sb - 2$ where $s = 1$ or 2 since $0 \leq i \leq b - 1$.

$i_y = i_{p-y}$ for $s = 2$. But $i_y \neq i_{p-y}$ for $p = \text{odd}$, hence $s = 1$. Thus:

$$a^* + b^* = i_y + i_{p-y} = b - 2.$$

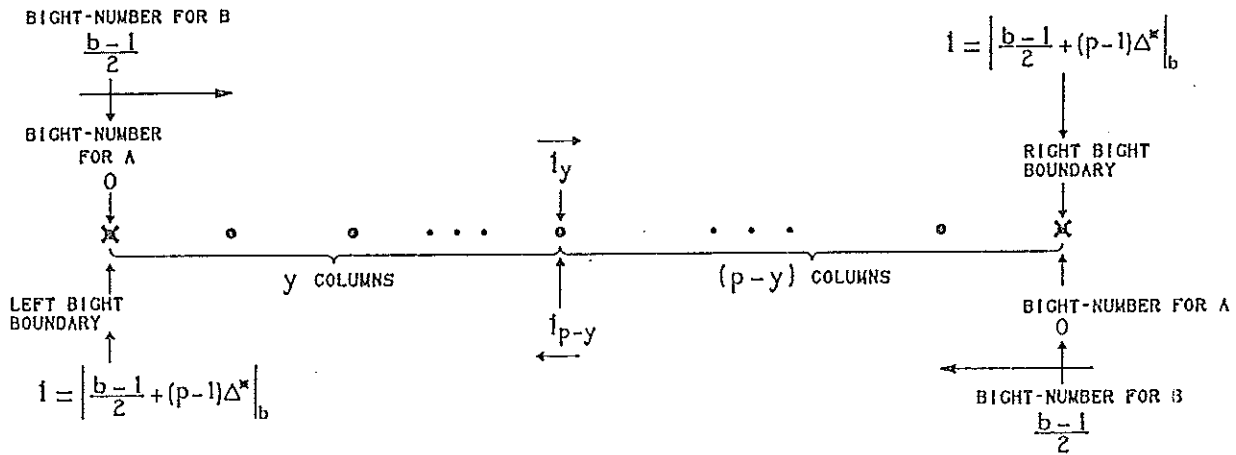


Fig. 319 — The general algorithm diagram for string B .

Question on pg. 366.

Let's first consider the case $p_m = 4n$; $b_m = 4m + 2$ where n and m are whole numbers.[†]

Let again string-run A be the real string-run and let string-run B be the imaginary string-run. Then the uppermost diagram in Fig. 320 depicts the complementary cyclic bight-number scheme for string A . Note that since the g.c.d. $(p, b) = 2$, the bight-points of string A are not the bight-points of string B , and we know from the g.c.d. value that the bight-points at either side of the bight-point at which string A starts are bight-points of string B . The bight-point at which the imaginary half-cycle of higher order of string B starts (bight-index number 0 for string B) receives in the complementary cyclic bight-number scheme the bight-number 0. Since $p = p_m$ and $b = b_m$, this bight-point lies $(\frac{b}{2} - \frac{p}{2}) = (2m - 2n + 1)$ bight-units to the right of the bight-point at which string A starts. Thus the bight-point immediately to the right of the bight-point at which string A starts lies $(2m - 2n)$ bight-units to the left of the bight-point

[†] Whole numbers are the numbers 0, 1, 2, 3, ...

Natural numbers or positive integers are the numbers 1, 2, 3, ...

Integers are the numbers ..., -3, -2, -1, 0, 1, 2, 3, ...

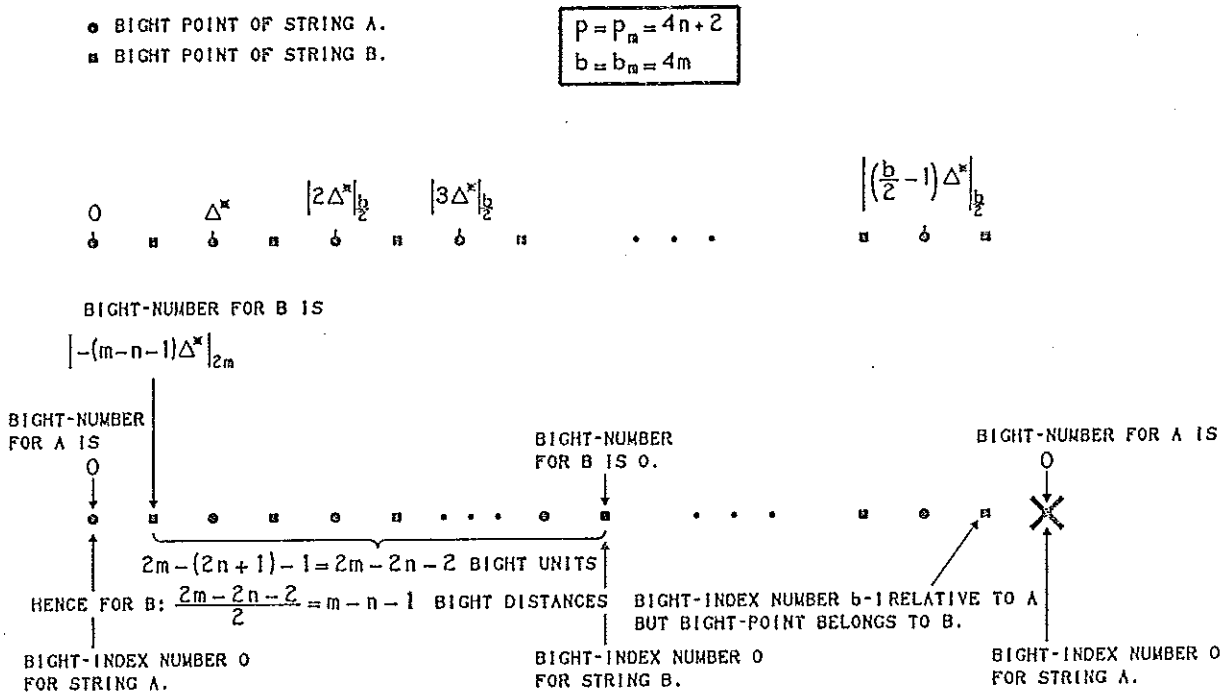


Fig. 321 — The complementary cyclic bight-number scheme for $p = p_m = 4n + 2 = \text{even}$ and $b = b_m = 4m = \text{even}$.

The general layout of the complementary cyclic bight-number scheme is shown in Fig. 322.

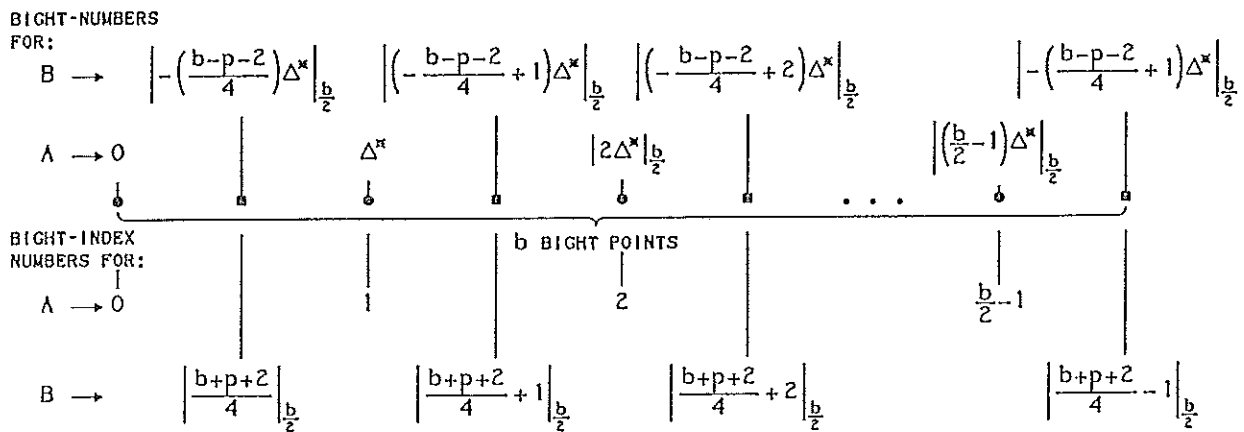


Fig. 322 — The complementary cyclic bight-number scheme for $p = p_m = \text{even}$ and $b = b_m = \text{even}$ with $\text{g.c.d.}(2p_m, [p_m + b_m]) = 2$.

Let for the imaginary string-run (hence string-run B) $i_y = a^*$ and $i_{\frac{b}{2}-y-1} = b^*$. Then for the case $p_m = 4n$; $b_m = 4m + 2$, where n and m are whole numbers, we obtain (see Fig. 323):

$$\begin{aligned}
 |i_y + i_{\frac{b}{2}-y-1}|_{\frac{b}{2}} &= |i_y + i_{2n-y-1}|_{\frac{b}{2}} \\
 &= |[-(m-n) + y]\Delta^*|_{2m+1} + |[-(m-n) + 2n - 1 - y]\Delta^*|_{2m+1}|_{2m+1}
 \end{aligned}$$

$$\begin{aligned}
 \left| i_y + i_{\frac{p}{2}-y-1} \right|_{\frac{b}{2}} &= |[-2m + 2n + (2n - 1)]\Delta^*|_{2m+1} \\
 &= |-(2m + 1)\Delta^* + 4n\Delta^*|_{2m+1} \\
 &= |4n\Delta^*|_{2m+1}; \text{ with } \Delta^* = \frac{b' \cdot \Delta_{II,1} p' - 1}{p'}, \text{ where } p' = \frac{p}{2}, b' = \frac{b}{2} : \\
 &= |-2|_{2m+1} = 2m - 1 = \frac{b}{2} - 2 = b' - 2.
 \end{aligned}$$

$$i_y + i_{\frac{p}{2}-y-1} = sb' - 2 \quad \text{where } s = 1 \text{ or } 2 \text{ since } 0 \leq i \leq b' - 1.$$

$$i_y = i_{\frac{p}{2}-y-1} \text{ for } s = 2.$$

But $i_y \neq i_{\frac{p}{2}-y-1}$ since $2y = \text{even} \neq 2n - 1 = \text{odd}$, hence $s = 1$. Thus:

$$a^* + b^* = i_y + i_{\frac{p}{2}-y-1} = b' - 2 = \frac{b}{2} - 2.$$

- COLUMNS A.
- COLUMNS B.

$$\begin{aligned}
 p &= p_m = 4n \\
 b &= b_m = 4m + 2
 \end{aligned}$$

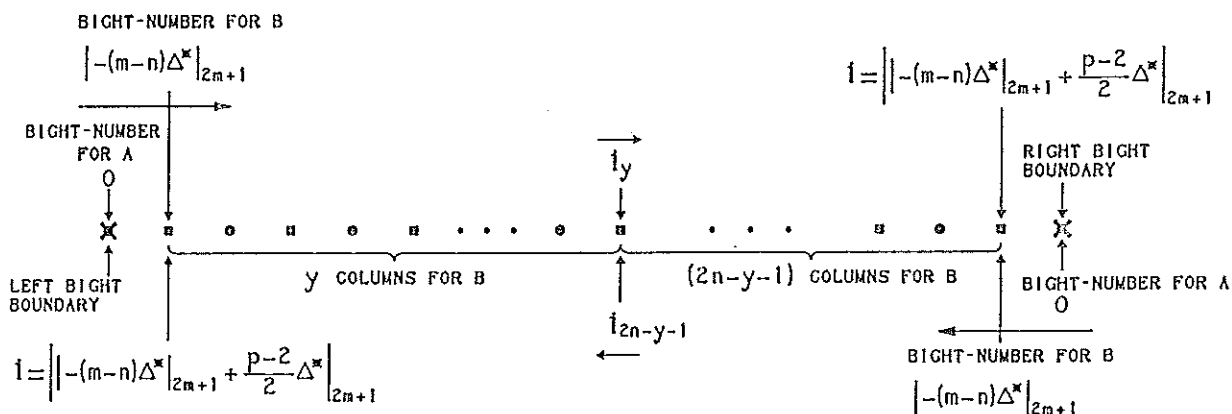


Fig. 323 — The general algorithm diagram for string B.

For the case $p_m = 4n + 2$; $b_m = 4m$, where n and m are whole numbers, we obtain (see Fig. 324):

- COLUMNS A.
- COLUMNS B.

$$\begin{aligned}
 p &= p_m = 4n + 2 \\
 b &= b_m = 4m
 \end{aligned}$$

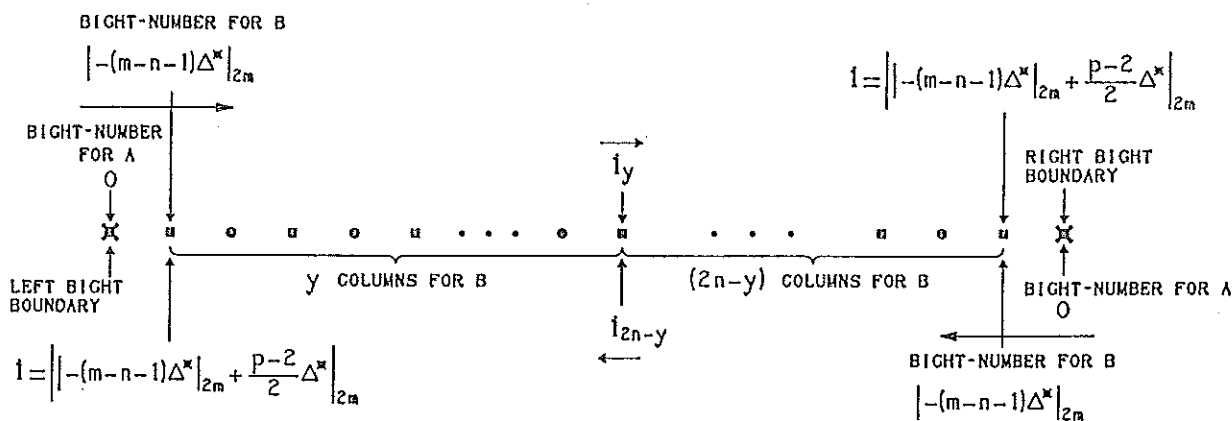


Fig. 324 — The general algorithm diagram for string B.

$$\begin{aligned}
 \left| i_y + i_{\frac{p}{2}-y-1} \right|_{\frac{b}{2}} &= |i_y + i_{2n-y}|_{\frac{b}{2}} \\
 &= |[-(m-n-1) + y]\Delta^*|_{2m} + |[-(m-n-1) + 2n-y]\Delta^*|_{2m}|_{2m} \\
 &= |[-2m + 2n + 2 + 2n]\Delta^*|_{2m} \\
 &= |(4n+2)\Delta^*|_{2m}; \text{ with } \Delta^* = \frac{b' \cdot \Delta_{II,1} p' - 1}{p'}, \text{ where } p' = \frac{p}{2}, b' = \frac{b}{2} : \\
 &= |-2|_{2m} = 2m - 2 = \frac{b}{2} - 2 = b' - 2.
 \end{aligned}$$

$$i_y + i_{\frac{p}{2}-y-1} = s b' - 2 \quad \text{where } s = 1 \text{ or } 2 \text{ since } 0 \leq i \leq b' - 1.$$

$$i_y = i_{\frac{p}{2}-y-1} \text{ for } s = 2. \text{ Hence } 2y = 2n, \text{ consequently } y = n.$$

It follows from the path in the RKT with its associated parities that Δ^* is odd (see Fig. 325).

$$\begin{aligned}
 p &= p_m = 4n + 2 \\
 b &= b_m = 4m
 \end{aligned}$$

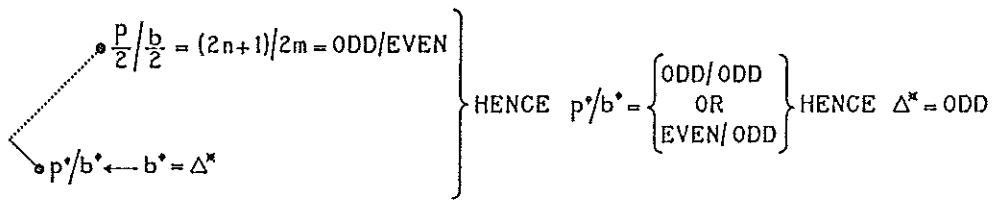


Fig. 325 — The parity of Δ^* in association with $p = p_m = 4n + 2$ and $b = b_m = 4m$.

Say $\Delta^* = 2t + 1$, then for $y = n$ we obtain:

$$\begin{aligned}
 i_y = i_n &= |[-(m-n-1) + n]\Delta^*|_{2m} \\
 &= |(-m + 2n + 1)\Delta^*|_{2m}; \text{ with } \Delta^* = \frac{b' \cdot \Delta_{II,1} p' - 1}{p'} = \frac{2m \cdot \Delta_{II,1} p' - 1}{2n + 1} : \\
 &= |-m\Delta^* - 1|_{2m}; \text{ with } \Delta^* = 2t + 1 : \\
 &= |-m - 1|_{2m} = m - 1. \text{ But } m - 1 < 2m - 1, \text{ hence } s \neq 2. \text{ Thus :} \\
 a^* + b^* &= i_y + i_{\frac{p}{2}-y-1} = b' - 2 = \frac{b}{2} - 2.
 \end{aligned}$$

Hence for $p = p_m = \text{even}$ and $b = b_m = \text{even}$ with $\text{g.c.d.}(2p_m, [p_m + b_m]) = 2$ we obtain for string B that $a^* + b^* = \frac{b_m}{2} - 2$.

Regular Cylindrical Bihelix Braids

In contrast with the Regular Cylindrical Braids, which have for the left to right half-cycles the same helix angle as for the right to left half-cycles, the Regular Cylindrical Bihelix Braids have for those respective half-cycles a different angle.

Just as a Cylindrical Knot may be regarded as a finite length of Round Braid with a minimum number of free string-ends, so may a Cylindrical Bihelix Knot be regarded as a finite length of Round Bihelix Braid with a minimum number of free string-ends.[†] Due to the different helix angles for the respective left to right and the right to left half-cycles, the weaving pattern will always have a spiral effect. This spiral effect in the Cylindrical Bihelix Knots will of course influence their string-run diagrams by making them somewhat more complicated. Hence let's first see how their string-run diagrams are constructed.

The two uppermost diagrams in Fig. 326 show the essential construction process for the string-run of a $[3, 7]$ Round Bihelix Braid. That is a Round Bihelix Braid which has 3 leads with a left-hand helix and 7 leads with a right-hand helix. In the uppermost left-hand diagram we did set off 3 unit-lengths horizontally followed by 7 unit-lengths vertically. Then we connected the starting-point with the end-point, thus creating the right-angled triangle. In this triangle the basic grid is produced by the vertical and horizontal lines through the points set off. Next we draw lines perpendicular to the hypotenuse through its end-points. Finally, about an axis through the lower vertex of this right-angled triangle we rotate in the clockwise direction the obtained diagram through an angle of $\arctan 3/7 = 23.1986^\circ$.[‡] This gives us the uppermost right-hand diagram. By extending the grid in this uppermost right-hand diagram between the two parallel horizontal lines (which represent the cylinder generating line of section) we obtain the string-run of the $[3, 7]$ Round Bihelix Braid. Any two vertically aligned points on these two parallel horizontal lines represent the same single point on the cylinder generating line of section. A line between the two horizontal lines, connecting crossing-points from lower right to upper left, represents a bight-boundary line when these crossing-points on such a line are made into bight-points. Such a bight-boundary line will always have a slant in a Cylindrical Bihelix Braid.^{††} Here we find the very significant difference between the bight-boundaries of a Regular Cylindrical Bihelix Braid and a Regular Cylindrical Braid that in the former the end-points of a bight-boundary line don't coincide (the end-points are not vertically aligned), whereas in the latter they do coincide. In a Round Bihelix Braid a bight-boundary line is a segment of a column-helix, and in the $[3, 7]$ Round Bihelix Braid we got $\sigma = 4$ such column-helices since $|3 - 7| = 4 = \sigma$ (see Fig. 327). A Cylindrical Bihelix Braid is a Regular Cylindrical Bihelix Braid when in a finite length of Round Bihelix Braid the set of left-hand bights and the set of right-hand bights each lie in a not stacked fashion on one or more of σ adjacent bight-boundary lines. In Figs. 326 & 328 the set of left-hand bights and the set of right-hand bights of the Regular Cylindrical Bihelix Braid lie each on one bight-boundary line. Note that in this braid the left-hand bight-boundary line and the right-hand bight-boundary line do not both belong to the same column-helix. Of the four adjacent bight-boundary lines on the left-hand side in Fig. 327, the bight-boundary lines $\sigma_1, \sigma_2, \sigma_4$ each carry one bight, and of the four adjacent bight-boundary lines on the right-hand side the bight-boundary lines $\sigma_1, \sigma_2, \sigma_3$ each carry one bight.

[†] Recall that we can also regard a Cylindrical Knot as a length of Flat Braid wrapped around a cylinder with strings of opposite ends suitably joined. Although an in essence similar procedure may be used for a Cylindrical Bihelix Knot, it is not very suitable.

[‡] $\arctan x$ (also written as \tan^{-1}) is the arc of which the tangent is equal to x .

^{††} Only when both helix angles are the same is a bight-boundary line vertical and do we have a Regular Cylindrical Braid.

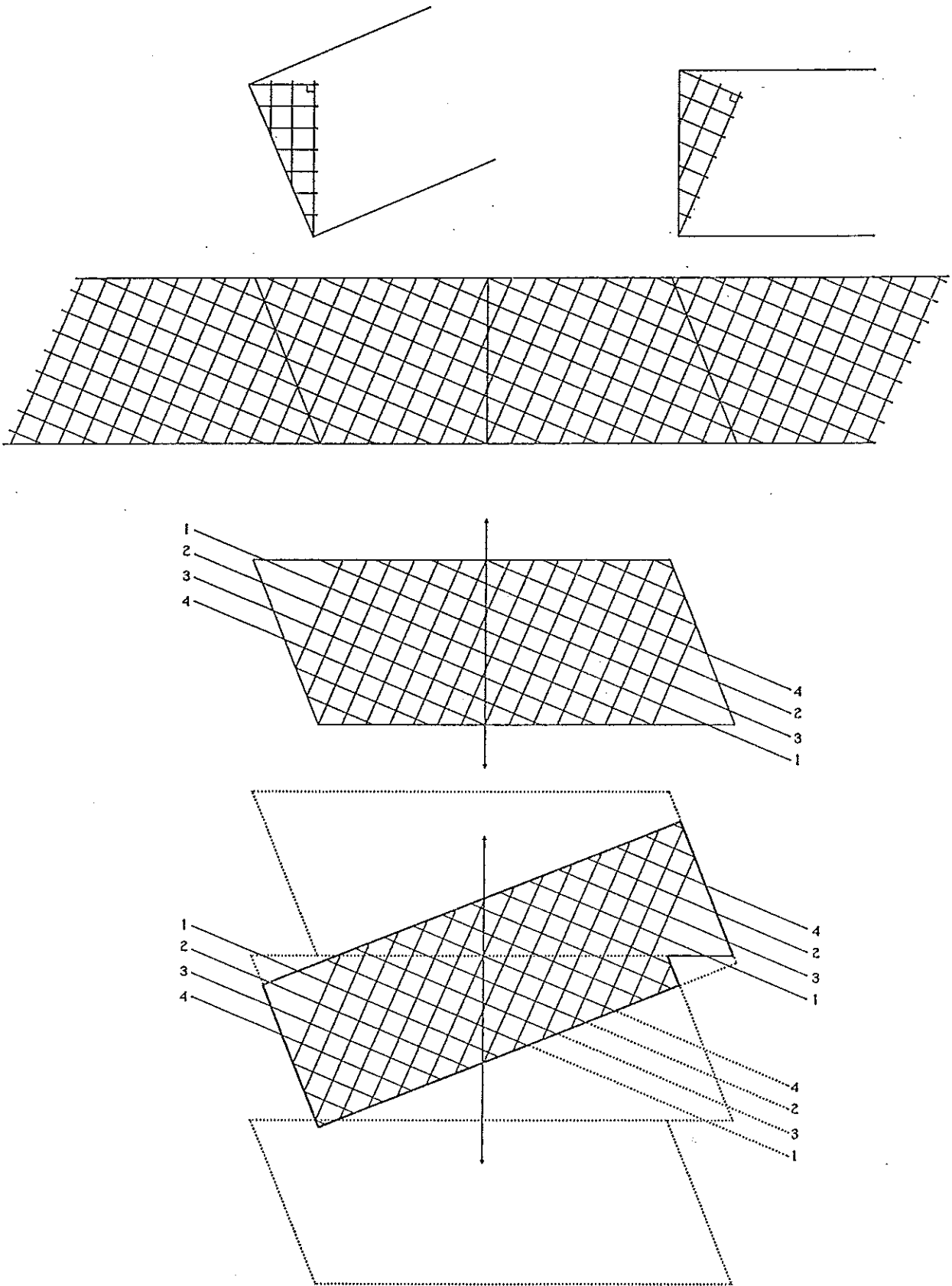


Fig. 326 — The string-run diagram of a $[3, 7]$ Bihelix Braid.

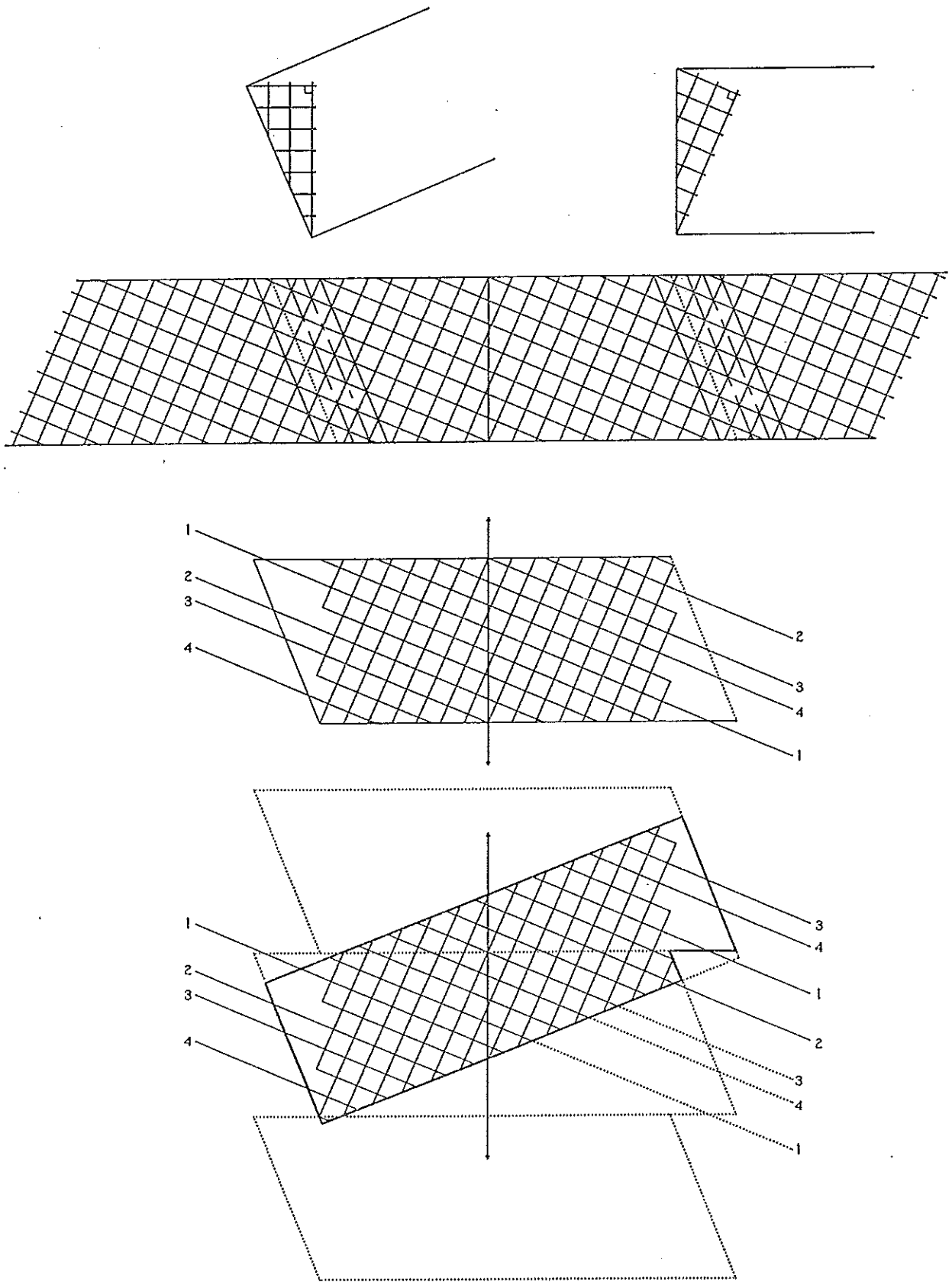


Fig. 327 — The string-run diagram of a $[3, 7]$ Bihelix Braid.

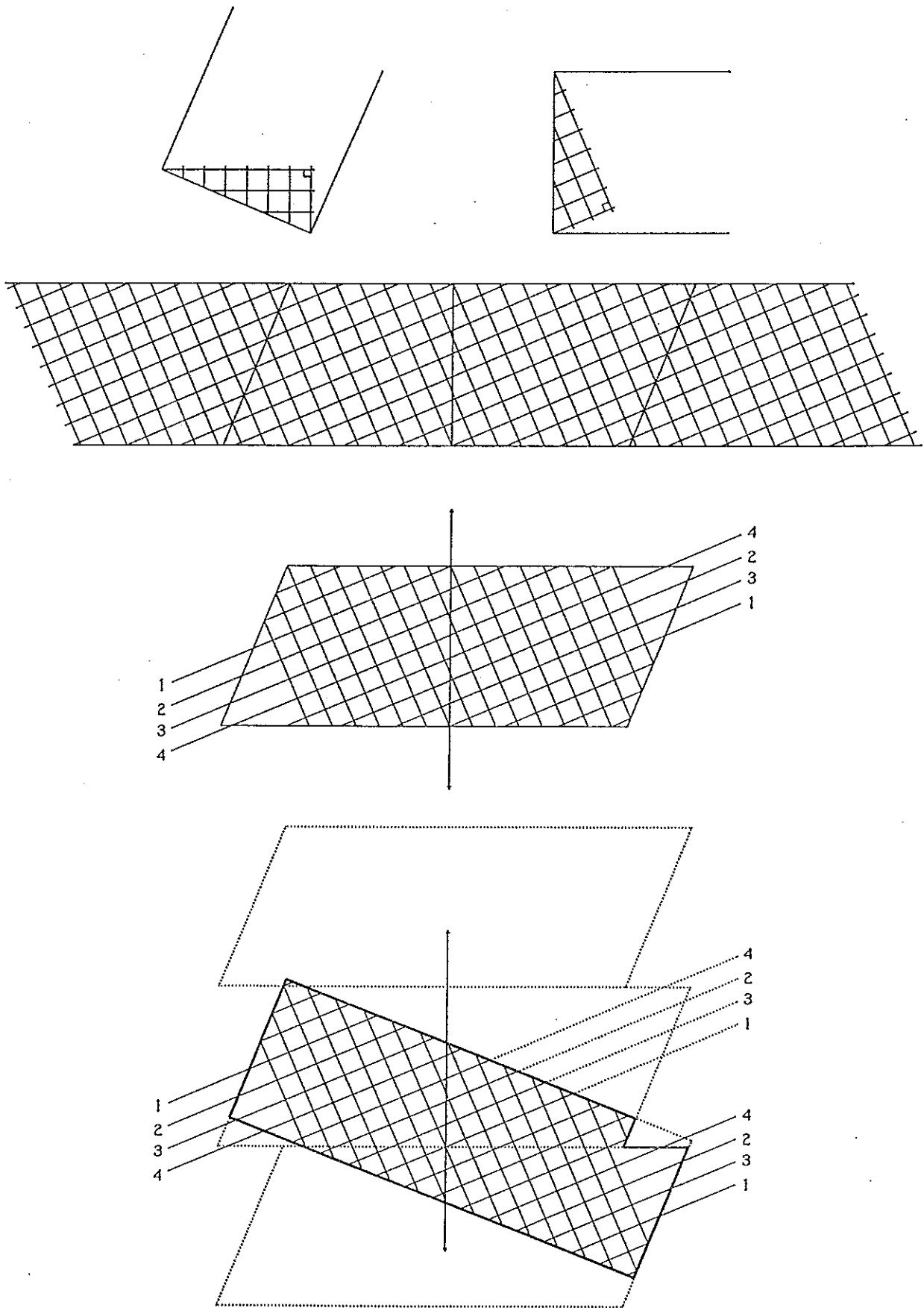


Fig. 328 — The string-run diagram of a $[7, 3]$ Bihelix Braid.

The essential construction process for the string-run of a $[7, 3]$ Round Bihelix Braid is shown in Fig. 328. That is a Round Bihelix Braid which has 7 leads with a left-hand helix and 3 leads with a right-hand helix. In the uppermost left-hand diagram we did set off 7 unit-lengths horizontally followed by 3 unit-lengths vertically. Then we connected the starting-point with the end-point, thus creating the right-angled triangle. In this triangle the basic grid is produced by the vertical and horizontal lines through the points set off. Next we draw lines perpendicular to the hypotenuse through its end-points. Finally, about an axis through the lower vertex of this right-angled triangle we rotate in the clockwise direction the obtained diagram through an angle of $\arctan 7/3 = 66.8014^\circ$ and extend the grid between the two horizontal lines.

The two horizontal lines (the cylinder generating line of section) of the Regular Cylindrical Bihelix Braids interfere with some string-run intersection-points and hence the lowermost modified string-run diagrams depicted in the Figs. 326-328 are often preferred.

In this Issue of *The Braider* we shall limit our discussion to the Round Bihelix Braids for which $\sigma = 1$, and as an Example of such a braid we shall take the $[11, 10]$ Round Bihelix Braid.

The construction of the string-run of this Round Bihelix Braid is shown in the upper part of Fig. 329. Since $\sigma = 1$, there is only one column-helix, and consequently there is only the σ_1 bight-boundary line.

Let's take the Regular Bihelix Knot depicted by the third row of diagrams in Fig. 329. The transfer of points between the top line and the bottom line in these diagrams is indicated by the vertical line with arrows at each of its ends. The half-cycles are numbered in the usual conventional way. The bottom row of diagrams in Fig. 329 depict exactly the same knot: only the cylinder generating line of section is in a different position!

Although in this Bihelix Knot both left and right bight-boundary lines start and end on the same cylinder generating line of section, the reader will no doubt realize that this is not a necessity. Hence for this reason alone (there is an other reason as well as we shall see a little later) we need to specify for a Bihelix Knot the number of its crossing-points. For the knot in Fig. 329 the number of crossing-points is 168.

After braiding this knot, the skewness indicated by the slanting bight-boundary lines will more or less disappear due to some automatic realignment. From the bottom row of diagrams it will be evident that the best possible realignment will be obtained when both the left and right bight-boundary lines start and end on the same cylinder generating line of section. Hence only those Regular Cylindrical Bihelix Braids whose left and right bight-boundary lines start and end on the same cylinder generating line of section will be called Prime Regular Cylindrical Bihelix Braids; the one string variety are then the Prime Regular Bihelix Knots.

In Fig. 330 are depicted the first 25 consecutive Prime Regular Cylindrical Bihelix Braids associated with the $[11, 10]$ Round Bihelix Braid. In the first 21 diagrams the number of column-lines increase in a regular manner by one in each consecutive diagram. Diagram #22, however, although having the same number of column-lines as diagram #21, has one more crossing-point (this is the other reason, referred to earlier, for specifying the number of crossing-points in order for unambiguously specifying a Prime Regular Cylindrical Bihelix Braid). This phenomenon will occur at regular intervals.

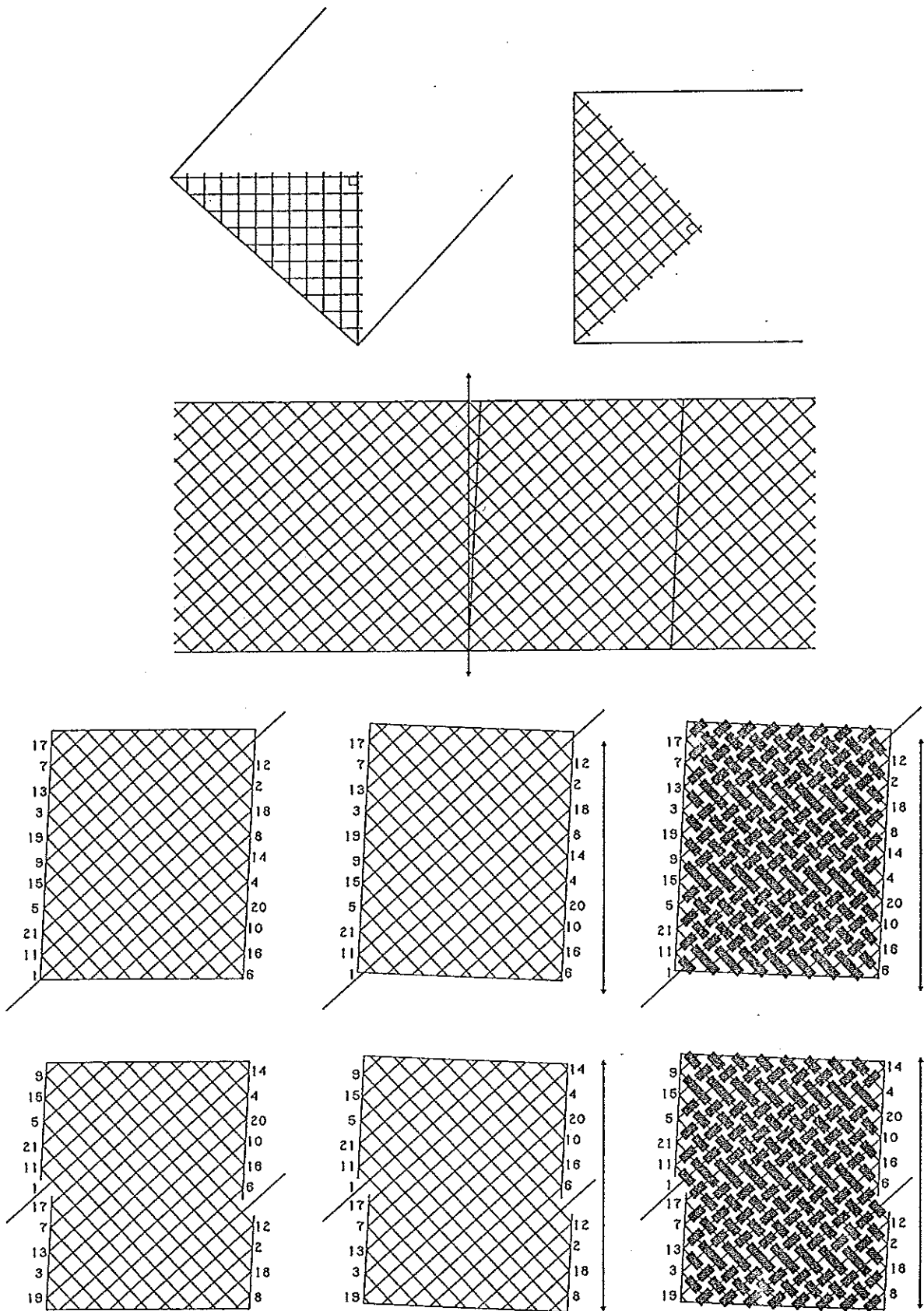


Fig. 329 — The string-run diagram of a [11, 10] Bihelix Braid.

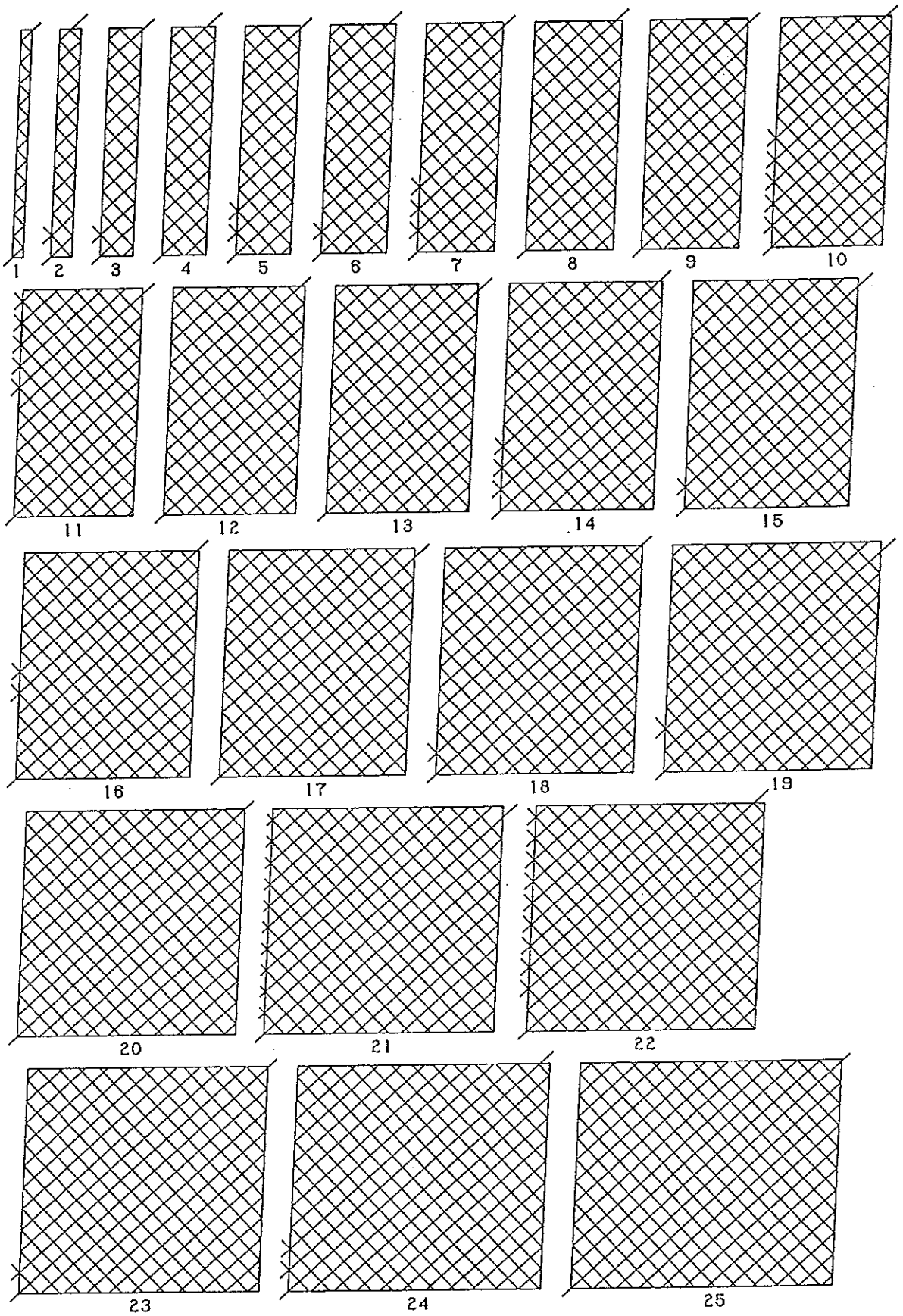


Fig. 330 — The first 25 consecutive Prime Regular Cylindrical [11, 10] Bihelix Braids.

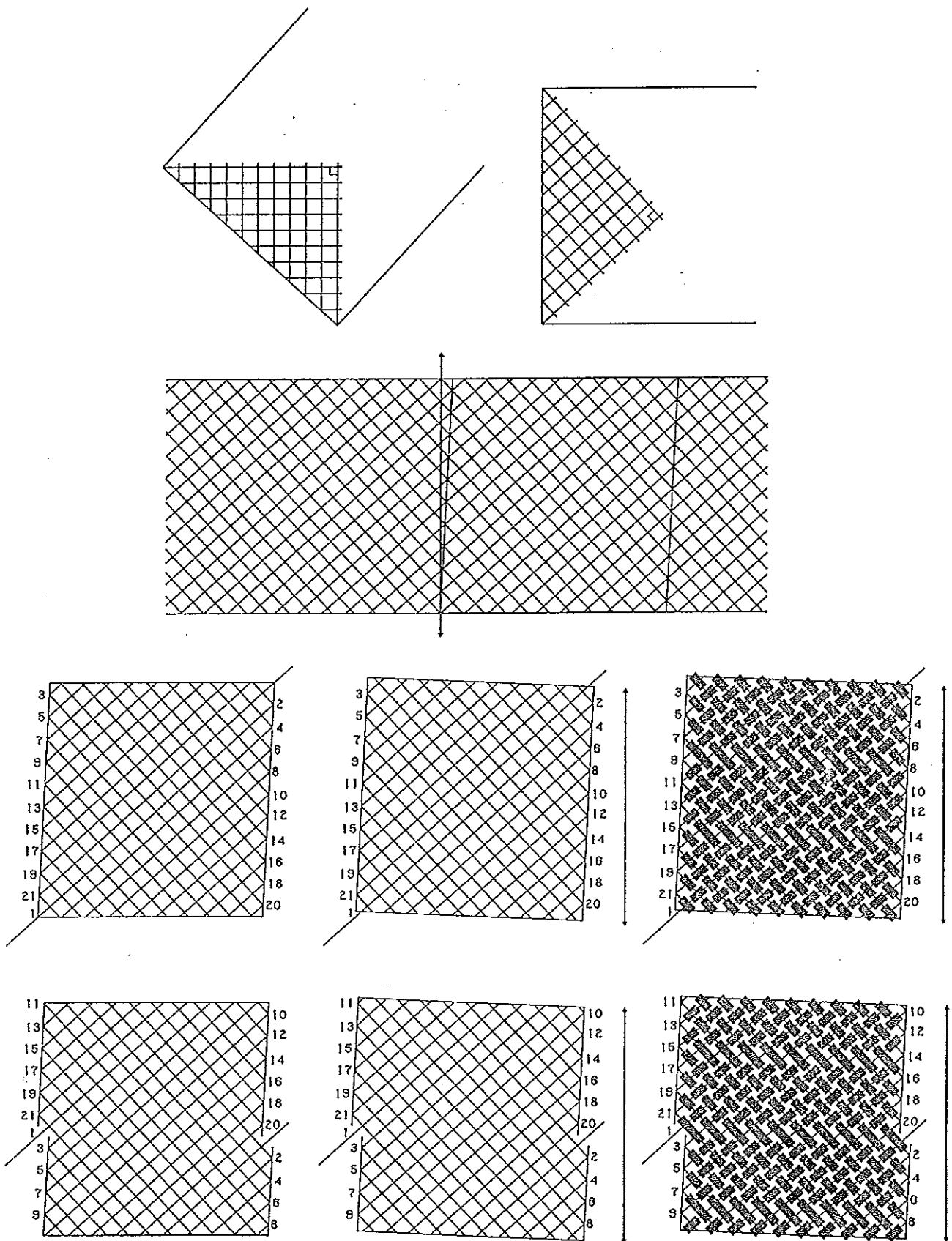


Fig. 331 — The Prime Regular $[11, 10]$ Bihelix Knot with 200 crossing-points.

In our Example it occurs for the first time between the Prime Regular Cylindrical Bihelix Braids with 210 crossing-points and 211 crossing-points, next it will occur between the Prime Regular Cylindrical Bihelix Braids with 431 and 432 crossing-points, next between the Prime Regular Cylindrical Bihelix Braids with 652 and 653 crossing-points, and so on. In due course we will meet these Prime Regular Cylindrical Bihelix Braids with 211, 431 and 653 crossing-points again in connection with another braid-form, and we shall then discuss the special properties they possess.

The Prime Regular Bihelix Knot in Fig. 331 has 200 crossing-points. Its string-run diagram is #20 in Fig. 330. This is another special knot. It is identical to the Regular Knot in Fig. 332 in which the last half-cycle has not been laid down. Regular Cylindrical Braids in which the last half-cycle of one of the string has not been laid down are called **Premature Regular Cylindrical Braids**.

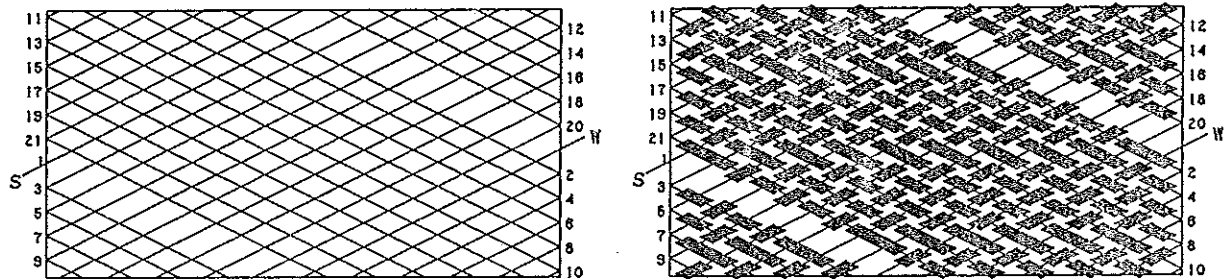


Fig. 332 — A $p/b = 21/11$ Premature Regular Knot.

Only a very few Premature Regular Cylindrical Braids are **Prime** Regular Cylindrical Bihelix Braids; in general they are only some of the Regular Cylindrical Bihelix Braids, an Example is shown in Fig. 333. Here the Premature Regular Cylindrical Braid is a Premature Regular Knot with 17-parts and 11-bights. It is identical to the Regular Bihelix Knot depicted by the second and third row diagrams in Fig. 333. It will readily be seen that a good realignment of the string-run is not possible. Consequently such knots should not be used in high class work.

In the string-run diagrams of Fig. 334 the dotted line depicts the missing last half-cycle of the Regular Cylindrical Braids having 11-bights. The bight-boundary line *A* is the bottom part of the right-hand bight-boundary line of the knot in the second row of diagrams of Fig. 333, and the bight-boundary line *B* is the right-hand bight-boundary line of the knot in Fig. 331. Note that between every two adjacent column-lines there is only one Regular Cylindrical Bihelix Braid (in most cases **not** Prime) which is equivalent to a Premature Regular Cylindrical Braid.

It will be evident that the string-run of a Prime Regular Cylindrical Bihelix Braid can be represented by an (in most cases) extended string-run diagram of a Regular Cylindrical Braid.

★★ From the sequence of diagrams in Fig. 335 explain the procedure used for constructing the diagrams. The same numbered diagrams in Figs. 335 and 330 depict the same braid.

We shall now have a brief look into the way we can calculate the number of string-run crossings of a Prime Regular Cylindrical $[(n + 1), n]$ Bihelix Braid.

Let N be the approximate number of crossing-points required, and let the **T-line** (see the diagrams of Fig. 335) be $\lfloor 2m + \lfloor \frac{m}{n} \rfloor \rfloor_{2(n+1)}$ rows (in cyclic fashion) above the **S-line** (the dotted line through the bight-point of the Standing End *S*).[†]

[†] $\lfloor x \rfloor$ denotes the greatest whole number equal to or smaller than x .

Then: $m = \left\lfloor \frac{N + n}{2n^2 + 2n + 1} \right\rfloor$.

Let $y = N + n - m(2n^2 + 2n + 1) = zn + r$, where $0 \leq r \leq n$.

Then we have the following three cases:[†]

$$\begin{array}{c} r < \left\lfloor \frac{z-1}{2} \right\rfloor \\ y_L^* = (z-1)n + \left\lfloor \frac{z-2}{2} \right\rfloor \\ y_H^* = zn + \left\lfloor \frac{z-1}{2} \right\rfloor \end{array} \left| \begin{array}{c} r > \left\lfloor \frac{z-1}{2} \right\rfloor \\ y_L^* = zn + \left\lfloor \frac{z-1}{2} \right\rfloor \\ y_H^* = (z+1)n + \left\lfloor \frac{z}{2} \right\rfloor \end{array} \right| \begin{array}{c} r = \left\lfloor \frac{z-1}{2} \right\rfloor \\ y^* = y = zn + \left\lfloor \frac{z-1}{2} \right\rfloor \end{array}$$

Then : $\left. \begin{array}{l} N_L = m(2n^2 + 2n + 1) - n + y_L^* \\ N_H = m(2n^2 + 2n + 1) - n + y_H^* \end{array} \right\}$ let N^* be the N selected, then :

$$\begin{aligned} N^* &= m(2n^2 + 2n + 1) - n + z^*n + \left\lfloor \frac{z^* - 1}{2} \right\rfloor \\ &= n \left(2mn + 2m + z^* - 1 + \left\lfloor \frac{m + \left\lfloor \frac{z^* - 1}{2} \right\rfloor}{n} \right\rfloor \right) + \left\lfloor m + \left\lfloor \frac{z^* - 1}{2} \right\rfloor \right\rfloor_n \\ &= n(p - 1) + \left\{ \left\lfloor m + \left\lfloor \frac{z^* - 1}{2} \right\rfloor \right\rfloor_n \right\} . \\ p &= 2mn + 2m + z^* + \left\lfloor \frac{m + \left\lfloor \frac{z^* - 1}{2} \right\rfloor}{n} \right\rfloor . \end{aligned}$$

Here p is the number of parts of the unextended Premature Regular Cylindrical Braid, which with its extension of $\left\{ \left\lfloor m + \left\lfloor \frac{z^* - 1}{2} \right\rfloor \right\rfloor_n \right\}$ bight-points (this are the extreme right-hand bights between the M-line and T-line) is equivalent to the Prime Regular Cylindrical $[(n + 1), n]$ Bihelix Braid with N^* crossings in its string-run.

Example 1 :

Say $N = 873$ and $n = 10$. Then: $2n^2 + 2n + 1 = 200 + 20 + 1 = 221$.

$$m = \left\lfloor \frac{N + n}{2n^2 + 2n + 1} \right\rfloor = \left\lfloor \frac{873 + 10}{221} \right\rfloor = \lfloor 3.996 \rfloor = 3 .$$

$$y = N + n - m(2n^2 + 2n + 1) = 220 = 22n + 0 = 21n + 10 = zn + r .$$

$$r = 10 = \left\lfloor \frac{21 - 1}{2} \right\rfloor = \left\lfloor \frac{z - 1}{2} \right\rfloor .$$

$$y^* = y = zn + \left\lfloor \frac{z - 1}{2} \right\rfloor = 21n + \left\lfloor \frac{21 - 1}{2} \right\rfloor = 21n + 10 = 220 .$$

$$N = m(2n^2 + 2n + 1) - n + y^* = 873 \rightarrow p = 88 ; \left\{ \left\lfloor m + \left\lfloor \frac{z^* - 1}{2} \right\rfloor \right\rfloor_n \right\} = 3 .$$

[†] $\lfloor x \rfloor$ denotes the smallest whole number equal to or greater than x .

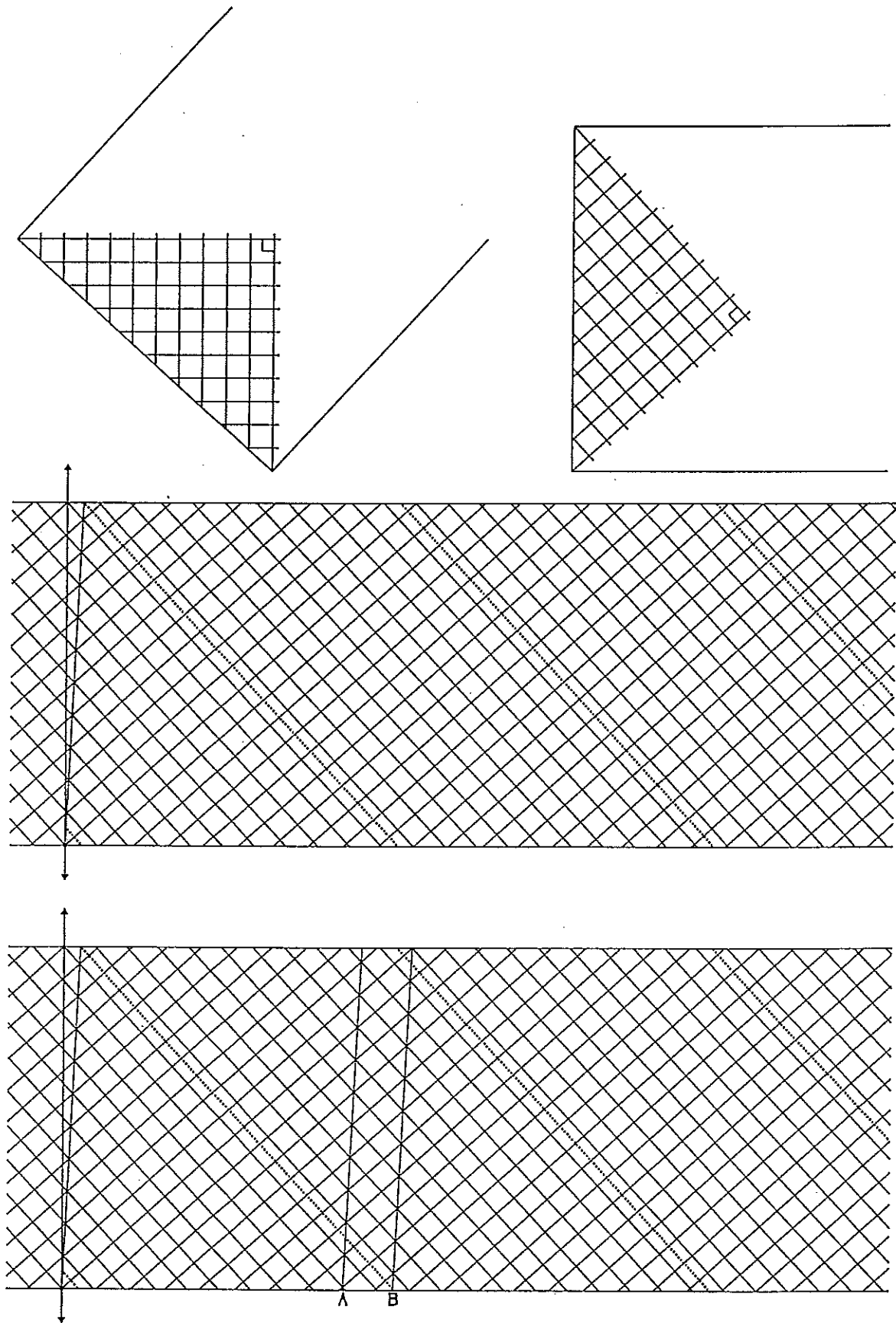


Fig. 334 - Premature Regular Cylindrical Braids in the [11, 10] Bihelix Round Braid.

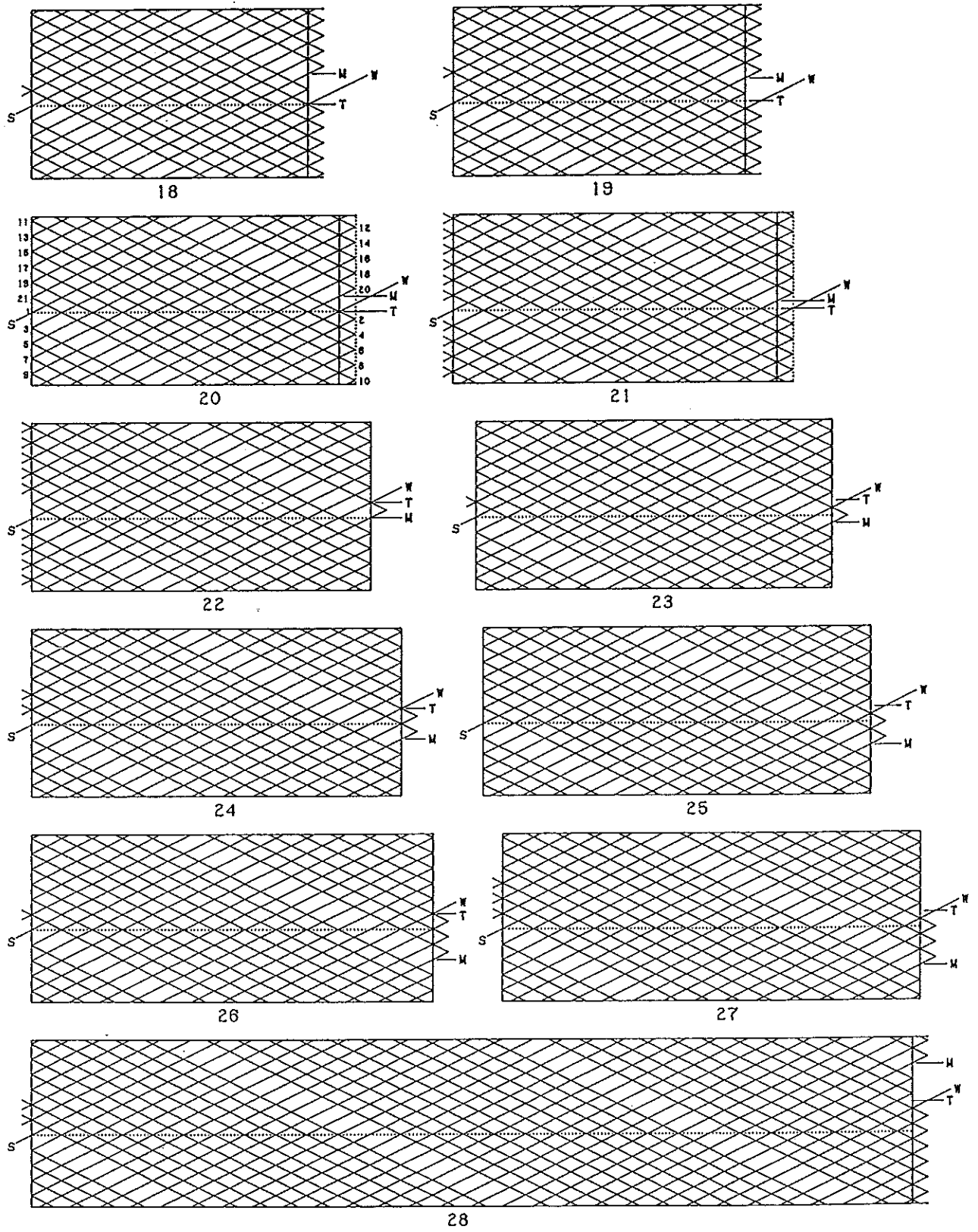


Fig. 335 — Prime Regular Cylindrical [11, 10] Bihelix Braids as extended Premature Regular Cylindrical Braids.

Example 3:

Say $N = 564$ and $n = 10$. Then: $2n^2 + 2n + 1 = 200 + 20 + 1 = 221$.

$$m = \left\lfloor \frac{N + n}{2n^2 + 2n + 1} \right\rfloor = \left\lfloor \frac{564 + 10}{221} \right\rfloor = [2.597] = 2.$$

$$y = N + n - m(2n^2 + 2n - 1) = 564 + 10 - 2 \cdot 221 = 132 = 13n + 2 = zn + r.$$

$$r = 2 < \left\lfloor \frac{13 - 1}{2} \right\rfloor = \left\lfloor \frac{z - 1}{2} \right\rfloor.$$

$$y_L^* = (z - 1)n + \left\lfloor \frac{z - 2}{2} \right\rfloor = (13 - 1)n + \left\lfloor \frac{13 - 2}{2} \right\rfloor = 12n + 6 = 126.$$

$$y_H^* = zn + \left\lfloor \frac{z - 1}{2} \right\rfloor = 13n + \left\lfloor \frac{13 - 1}{2} \right\rfloor = 13n + 6 = 136.$$

$$N_L = m(2n^2 + 2n + 1) - n + y_L^* = 558 \rightarrow p = 56; \left\{ \left\lfloor m + \left\lfloor \frac{z^* - 1}{2} \right\rfloor \right\rfloor_n \right\} = 8.$$

$$N_H = m(2n^2 + 2n + 1) - n + y_H^* = 568 \rightarrow p = 57; \left\{ \left\lfloor m + \left\lfloor \frac{z^* - 1}{2} \right\rfloor \right\rfloor_n \right\} = 8.$$

Example 4:

Say $N = 6842$ and $n = 10$. Then: $2n^2 + 2n + 1 = 200 + 20 + 1 = 221$.

$$m = \left\lfloor \frac{N + n}{2n^2 + 2n + 1} \right\rfloor = \left\lfloor \frac{6842 + 10}{221} \right\rfloor = [31.005] = 31.$$

$$y = N + n - m(2n^2 + 2n - 1) = 6842 + 10 - 31 \cdot 221 = 1 = 0n + 1 = zn + r.$$

$$r = 1 > \left\lfloor \frac{0 - 1}{2} \right\rfloor = \left\lfloor \frac{z - 1}{2} \right\rfloor = 0.$$

$$y_L^* = zn + \left\lfloor \frac{z - 1}{2} \right\rfloor = 0n + \left\lfloor \frac{0 - 1}{2} \right\rfloor = 0n + 0 = 0.$$

$$y_H^* = (z + 1)n + \left\lfloor \frac{z}{2} \right\rfloor = 1n + \left\lfloor \frac{0}{2} \right\rfloor = 1n + 0 = 10.$$

$$N_L = m(2n^2 + 2n + 1) - n + y_L^* = 6841 \rightarrow p = 685; \left\{ \left\lfloor m + \left\lfloor \frac{z^* - 1}{2} \right\rfloor \right\rfloor_n \right\} = 1.$$

$$N_H = m(2n^2 + 2n + 1) - n + y_H^* = 6851 \rightarrow p = 686; \left\{ \left\lfloor m + \left\lfloor \frac{z^* - 1}{2} \right\rfloor \right\rfloor_n \right\} = 1.$$

For the $[n, (n + 1)]$ Prime Regular Cylindrical Bihelix Braids we obtain of course exactly the same general formulae since their string-runs are the mirror image of the $[(n + 1), n]$ Prime Regular Cylindrical Bihelix Braids.

We can also obtain for the Prime Regular Cylindrical Bihelix Braids their equivalent extended Premature Regular Cylindrical Braids by means of the position of the M-line in relation to the the position of the T-line. This is the more graphical method associated with the question on pg. 387.

Although the grid-diagrams of the extended Premature Regular Cylindrical Braids do not give us a good picture of the actual braid (only the proper bihelix diagrams are able to do this), they are nevertheless of great value not only for the actual construction process employed but also as an aid in the derivation of the half-cycle algorithms.